

# CRUCIAL ROLE OF THE MEMBRANE POTENTIAL FOR ATP SYNTHESIS BY F<sub>1</sub>F<sub>0</sub> ATP SYNTHASES

PETER DIMROTH\*, GEORG KAIM AND ULRICH MATTHEY

*Institut für Mikrobiologie, Eidgenössische Technische Hochschule, ETH-Zentrum, Schmelzbergstraße 7, CH-8092 Zürich, Switzerland*

\*e-mail: dimroth@micro.biol.ethz.ch

*Accepted 18 October; published on WWW 13 December 1999*

## Summary

ATP, the universal carrier of cell energy, is manufactured from ADP and phosphate by the enzyme ATP synthase using the free energy of an electrochemical gradient of protons (or Na<sup>+</sup>). The proton-motive force consists of two components, the transmembrane proton concentration gradient ( $\Delta\text{pH}$ ) and the membrane potential. The two components were considered to be not only thermodynamically but also kinetically equivalent, since the chloroplast ATP synthase appeared to operate on  $\Delta\text{pH}$  only. Recent experiments demonstrate, however, that the chloroplast ATP synthase, like those of mitochondria and

bacteria, requires a membrane potential for ATP synthesis. Hence, the membrane potential and proton gradient are not equivalent under normal operating conditions far from equilibrium. These conclusions are corroborated by the finding that only the membrane potential induces a rotary torque that drives the counter-rotation of the a and c subunits in the F<sub>0</sub> motor of *Propionigenium modestum* ATP synthase.

Key words: F<sub>1</sub>F<sub>0</sub> ATP synthase, F<sub>0</sub> motor, intersubunit rotation, membrane potential, torque generation, *Propionigenium modestum*.

## Introduction

According to Mitchell's chemiosmotic hypothesis, the respiratory chain converts redox energy into an electrochemical gradient of protons (proton-motive force,  $\Delta\text{p}$ ) which subsequently drives ATP formation from ADP and phosphate by the F<sub>1</sub>F<sub>0</sub> ATP synthase. The two parameters of  $\Delta\text{p}$  are the membrane potential ( $\Delta\psi$ ) and the transmembrane proton gradient ( $\Delta\text{pH}$ ), which are thermodynamically equivalent:

$$\Delta\text{p} = \Delta\psi + 2.3RT/F\Delta\text{pH},$$

where  $R$  is the gas constant,  $T$  is absolute temperature and  $F$  is Faraday's constant.

The contribution of either parameter to the proton-motive force varies widely in different organisms. In mitochondria, the  $\Delta\psi$  component significantly exceeds the  $\Delta\text{pH}$  component and is therefore regarded as the main driving force for ATP production. In contrast, chloroplasts appear to operate mainly on  $\Delta\text{pH}$  which, at approximately 3 pH units in the steady state, far exceeds the  $\Delta\psi$  of  $\leq 50$  mV (Gräber and Witt, 1976). Bacteria are remarkably flexible and are able to grow in environments with a wide range of pH values. Extreme species are the alkaliphiles and acidophiles, which have specialised to grow at pH values above 10 or below 4, respectively. For the alkaliphiles, which keep their internal pH at around 8.5, the membrane potential not only serves as the exclusive thermodynamic driving force for ATP synthesis, but it also has to compensate for the counteracting inverse  $\Delta\text{pH}$ . In spite of

these variations, there is a remarkable similarity in the phosphorylation potentials, i.e. the [ATP]/[ADP][phosphate] ratios, in the various organisms (Hoffmann and Dimroth, 1991; Krulwich, 1995).

Hence, thermodynamically, both parameters of the proton-motive force undoubtedly contribute driving forces for the synthesis of ATP according to equation 1. However, this equilibrium equation says nothing about how the two components contribute to the kinetics of ATP formation during normal operation; this depends on the mechanism of energy conversion. Important early studies reported on ATP synthesis by thylakoid membranes energised with either  $\Delta\text{pH}$  or  $\Delta\psi$  (Jagendorf and Uribe, 1966; Uribe, 1973), and similar results were obtained using submitochondrial particles (Thayer and Hinkle, 1975). These results were corroborated and extended with the reconstituted ATP synthases of chloroplasts or other sources, leading to the conclusion that  $\Delta\text{pH}$  and  $\Delta\psi$  are not only thermodynamically but also kinetically equivalent driving forces for the synthesis of ATP (Junesch and Gräber, 1991; Turina et al., 1991). However, these results have recently been challenged: it was shown that the 'acid bath procedure' used in all these experiments not only generates the desired  $\Delta\text{pH}$  but also a  $\Delta\psi$  of significant size (Kaim and Dimroth, 1998a, 1999). Remarkably, the ATP synthase of chloroplasts or *Escherichia coli* is dependent on the  $\Delta\psi$  component, because no ATP synthesis can be measured in its absence in spite of considerable  $\Delta\text{pH}$  values. Here, we will give a detailed account of the essential importance

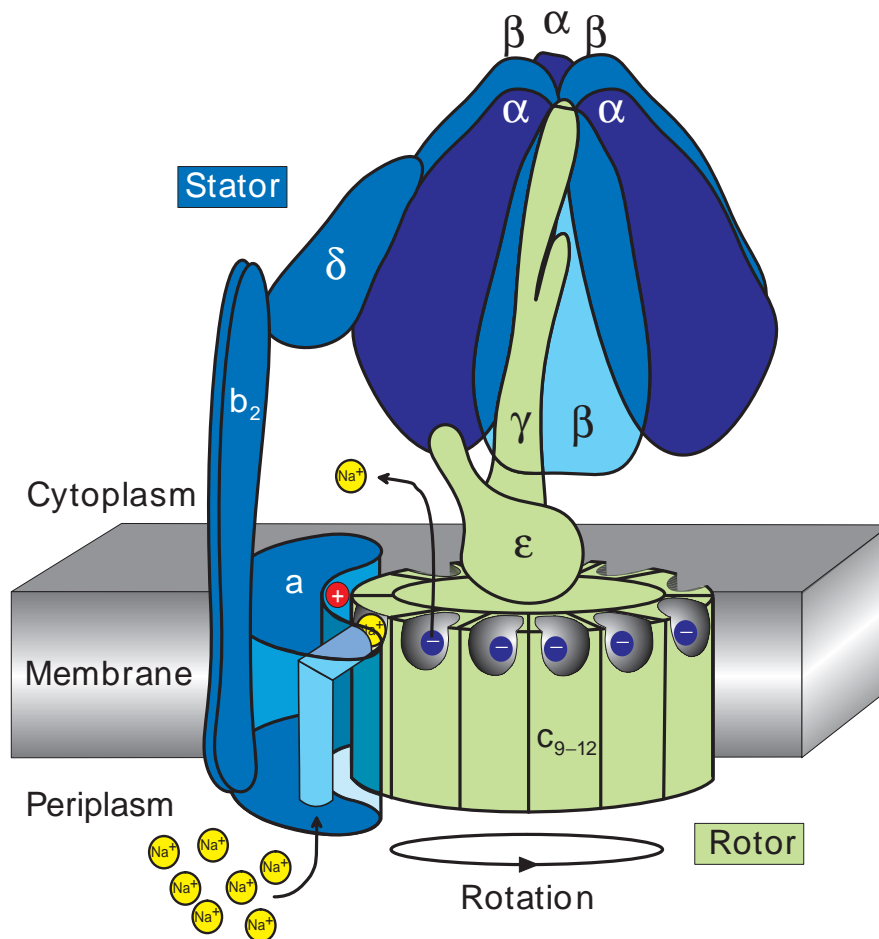


Fig. 1. Cartoon showing the structure and function of the *Propionigenium modestum* ATP synthase. The water-soluble  $F_1$  domain with the catalytic sites on the three  $\beta$  subunits is connected *via*  $\gamma$  and  $\epsilon$  subunits with the c-ring ( $c_{9-12}$ ) of the  $F_0$  domain and *via*  $\delta$  and  $b_2$  subunits with the  $F_0$  subunit a. The rotor (green) consists of subunits  $c_{9-12}\gamma\epsilon$ , and the stator (blue) consists of subunits  $a\beta_2\alpha_3\beta_3\delta$ . The path of  $\text{Na}^+$  during ATP synthesis is from the periplasm through the a subunit channel onto an empty c subunit site at the rotor–stator interface. After the rotor site has been moved out of the interface with the stator, the  $\text{Na}^+$  dissociates into the cytoplasm. The positive stator charge (aR227, red), which electrostatically attracts empty, negatively charged rotor sites (cE65, dark blue), is indicated.

of the membrane potential in generating rotational torque by the  $F_0$  motor. This torque is required to liberate, *via* rotation of the  $\gamma$  subunit, tightly bound ATP from catalytic sites in  $F_1$ .

### The $\text{Na}^+$ ( $\text{Li}^+$ or $\text{H}^+$ )-translocating ATP synthase of *Propionigenium modestum*

The  $F_1F_0$  ATP synthases comprise a huge family of enzymes with members found in the bacterial cytoplasmic membrane, the inner membrane of mitochondria and the thylakoid membrane of chloroplasts. Although most members of this family use  $\text{H}^+$  as the exclusive coupling ion, the *P. modestum* enzyme is the prototype of a few ATP synthases that use  $\text{Na}^+$  as the physiological coupling ion and switch to  $\text{Li}^+$  or  $\text{H}^+$  under certain conditions (Dimroth, 1997). We will see below that just a few amino acid substitutions in the a and c subunits determine changes in coupling ion specificity and that the overall structure and function of the  $\text{H}^+$ - and  $\text{Na}^+$ -translocating ATP synthases are the same. This has been most convincingly demonstrated by combining subunits of the  $\text{H}^+$ -translocating *E. coli* ATP synthase with those of the  $\text{Na}^+$ -translocating *P. modestum* ATP synthase to form functional chimeras (Kaim and Dimroth, 1993).

Fig. 1 shows the overall geometry of the *P. modestum* ATP synthase. The structure is divided into the membrane-integral  $F_0$  moiety, comprising subunits  $a\beta_2c_{9-12}$ , and the peripheral  $F_1$

part, composed of subunits  $\alpha_3\beta_3\gamma\delta\epsilon$ . For our purposes, we need only recognise that the entire structure can be subdivided into two counter-rotating assemblies denoted by convention as rotor and stator. The rotor consists of a ring of 9–12 c subunits connected to a shaft consisting of the  $\gamma$  and  $\epsilon$  subunits. The remainder of the assembly consists of subunits  $a\beta_2\alpha_3\beta_3\delta$  and is the stator. During ATP synthesis, the  $F_0$  motor converts the energy stored in a transmembrane electrochemical gradient of  $\text{Na}^+$  (or  $\text{H}^+$ ) into rotary torque (Kaim and Dimroth, 1998b). This drives the rotation of the  $\gamma$  subunit, eliciting conformational changes in the catalytic  $\beta$  subunits so that tightly bound ATP is released. In its reverse operation, the engine acts as an ATP-driven  $\text{Na}^+$  or  $\text{H}^+$  pump. Rotation of the  $\gamma$ ,  $\epsilon$  and c-ring assembly is now driven by the hydrolysis of ATP, and this rotation forces  $\text{Na}^+$  (or  $\text{H}^+$ ) to pass from the c subunit binding site through the a subunit channel to the other side of the membrane.

### Structural features of the membrane-bound rotor and stator subunits

As the atomic structure of  $F_0$  has not yet been resolved, one is restricted to understanding its function from low-resolution images, from the topological arrangements of the a and c subunits, from solution structures of the c subunit monomer

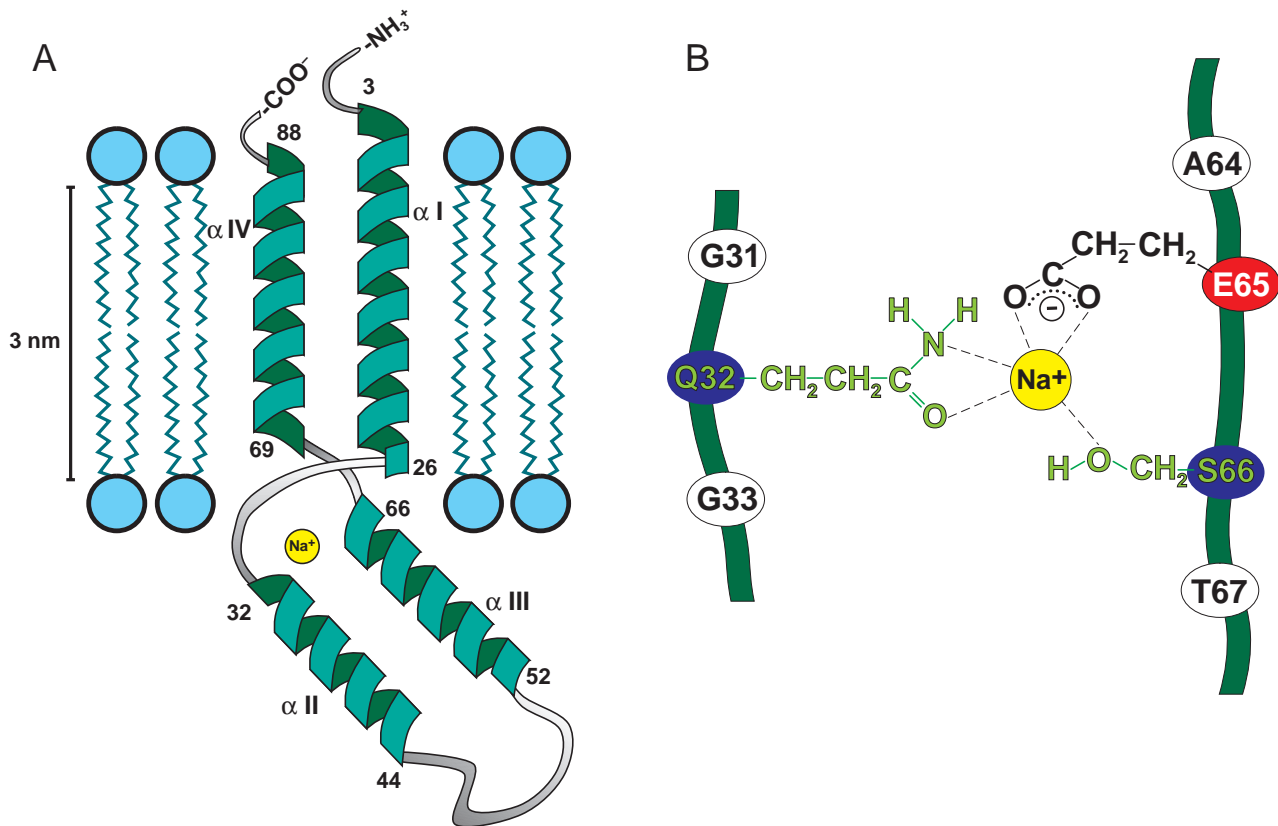


Fig. 2. (A) Model for insertion of *Propionigenium modestum* subunit c into the membrane. Helices I ( $\alpha$  I; 24 residues) and IV ( $\alpha$  IV; 18–20 residues) span the membrane, and helices II ( $\alpha$  II; 13 residues) and III ( $\alpha$  III; 15 residues) and the connecting loop of seven amino acid residues are exposed to the cytoplasm. The  $\text{Na}^+$ -binding site is located in the region of irregular secondary structure between helices I and IV and helices II and III and comprises residues of the N-terminal as well as the C-terminal sections of the polypeptide chain (Q32, E65, S66). The  $\text{Na}^+$ -binding site thus lies near the cytoplasmic membrane surface. This location is in accord with biochemical data indicating free access of this site for  $\text{Na}^+$  from the cytoplasm. (B) Details of the  $\text{Na}^+$  coordination sphere with ligands contributed by Q32, E65 and S66. Only residues E65 and S66 are required for  $\text{Li}^+$  binding, and E65 is the only residue required for  $\text{H}^+$  binding and translocation.

and from a variety of biochemical data. The overall structure of  $F_0$  inferred from electron and atomic force microscopy is that of a ring consisting of 9–12 copies of subunit c flanked at the periphery by one a and two b subunits (Birkenhäger et al., 1995; Singh et al., 1996; Takeyasu et al., 1996). Exceptionally stable c subunit assemblies are present in the ATP synthases from *P. modestum* (Laubinger and Dimroth, 1988) and *Ilyobacter tartaricus* (Neumann et al., 1998), in which even boiling with sodium dodecylsulphate (SDS) is not sufficient to dissociate the complex into monomers. The monomeric c subunits are conveniently isolated from whole cells by extraction with chloroform/methanol and fractionation on an ion-exchange column in mixed organic solvents. The c subunit contains only 80–90 amino acid residues and, therefore, structure determination by nuclear magnetic resonance (NMR) is feasible. In chloroform/methanol/ $\text{H}_2\text{O}$  (4:4:1), *E. coli* subunit c packs into two antiparallel  $\alpha$ -helices of 30–40 amino acid residues connected by a short hydrophilic loop (Girvin et al., 1998). Fillingame and colleagues proposed that the two extended  $\alpha$ -helices span the membrane, which places the  $\text{H}^+$ -binding D61 residue into an occluded position in the centre of

the bilayer (Girvin and Fillingame, 1994). The *P. modestum* subunit c, which was not stable in the organic solvent mixture, was subjected to NMR structure analysis in SDS micelles (Matthey et al., 1997). It was assumed that the detergent micelles mimic more closely the biphasic character of the membrane than the organic solvent mixture, which is monophasic. In the micelles, *P. modestum* subunit c folds into four clearly defined  $\alpha$ -helices connected by short peptides with non-regular secondary structures (Matthey et al., 1999) (Fig. 2A). The N-terminal and C-terminal helices were proposed to span the membrane, and the additional helices II and III and the intervening hydrophilic loop were proposed to protrude into the cytoplasm. In this structure, the  $\text{Na}^+$ -binding residues Q32, E65 and S66 (Kaim et al., 1997) are located in the helix I $\rightarrow$ II and helix III $\rightarrow$ IV connections, probably near the membrane surface on the cytoplasmic side. Hence, direct cytoplasmic access of these sites is readily conceivable, in accord with several lines of experimental evidence obtained with the ATP synthase of *P. modestum* (Kaim et al., 1998). Since structures have been conserved during evolution, it is not satisfactory that the two subunit c structures determined by

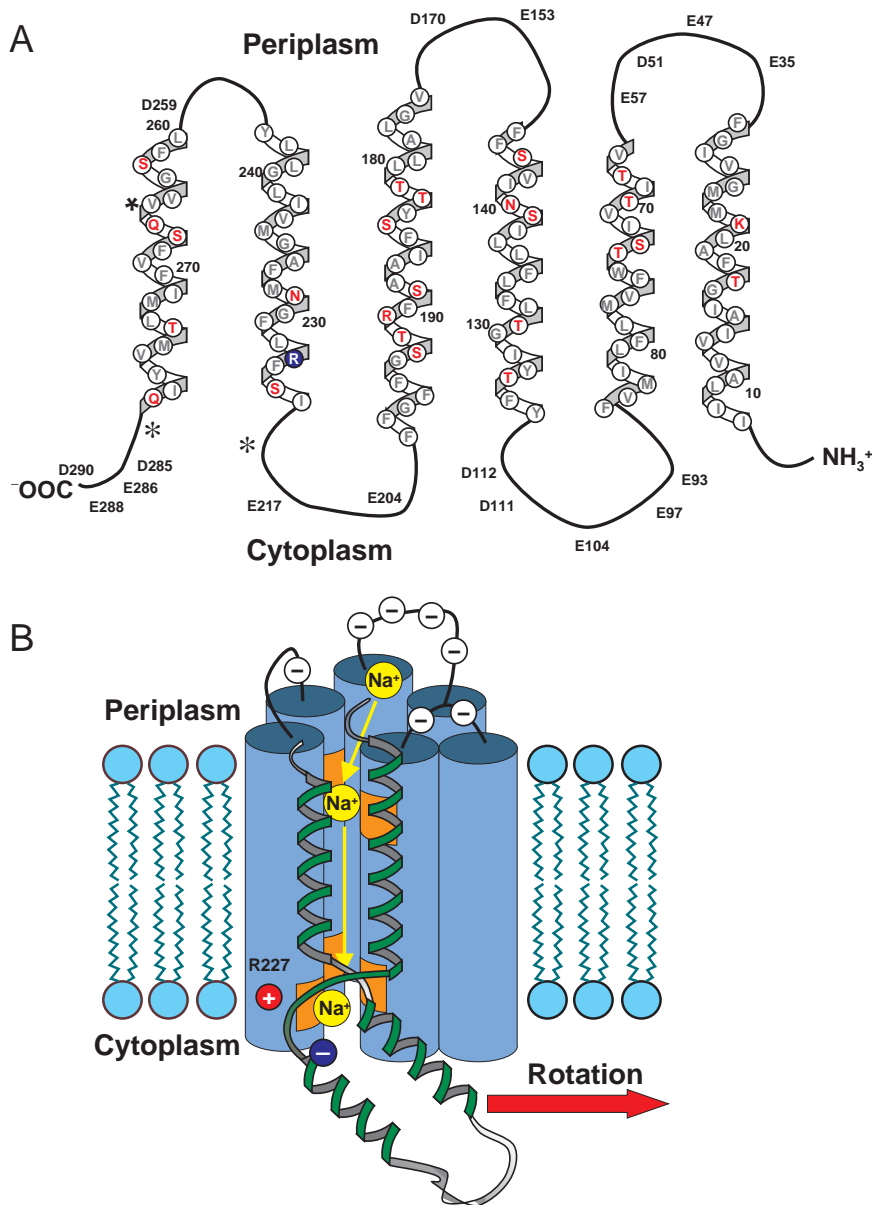


Fig. 3. (A) Sequence and putative topology of subunit a from *Propionigenium modestum*. Negatively charged residues are found exclusively in the cytoplasmic and periplasmic loops. The positive stator charge (R227, blue) is in close proximity to the cytoplasmic surface, where it interacts electrostatically with negatively charged rotor sites. Hydrophilic residues in putative transmembrane helices are coloured red. The three mutated residues leading to the  $\text{Na}^+$ -impermeable stator channel are marked (\*). (B) Detail of the rotor-stator assembly model as viewed from inside the rotor, showing the a subunit (blue cylinders) and a single rotor subunit (green helix). The location of the essential rotor (dark blue) and stator (red) charges and the path of  $\text{Na}^+$  into the stator helix bundle are also indicated. The ion channel terminates before penetrating all the way through the stator. The orange-coloured patches indicate polar hydrophilic regions. Rotation during ATP synthesis is to the right.

NMR are different. A reasonable explanation would be different folding patterns of the two proteins in the organic solvent mixture and in detergent micelles. It has been argued that the structure of *E. coli* subunit c in organic solvents closely mimics that in the native  $F_0$  complex because the specificity of D61 for dicyclohexylcarbodiimide (DCCD) was retained (Girvin and Fillingame, 1994). However, reduction of the modification rate by about four orders of magnitude makes this conclusion rather doubtful. *P. modestum* subunit c in dodecylsulphate micelles also retained its specificity for modification by DCCD (Matthey et al., 1997). The modification rate was approximately 10-fold lower than in the  $F_1F_0$  complex, and  $\text{Na}^+$  provided partial protection from DCCD labelling, indicating that the  $\text{Na}^+$ -binding site is retained in the detergent-solubilised c subunit monomer. However, even with these results, additional information is

needed to make a confident judgement about the structure of subunit c in its native folding pattern.

Probably the most important function of subunit c is to bind the coupling ions during their translocation across the membrane. For this purpose, each subunit c contains a binding site that specifically recognises the coupling ion(s). These features were first discovered for *P. modestum* subunit c, which may bind  $\text{Na}^+$ ,  $\text{Li}^+$  or  $\text{H}^+$  (Kluge and Dimroth, 1993a,b). Ligands for  $\text{Na}^+$  binding are provided by Q32, E65 and S66 (Fig. 2B), whereas E65 and S66 are sufficient for  $\text{Li}^+$  binding, and  $\text{H}^+$  binding depends entirely on E65 (Kaim et al., 1997). Consequently,  $\text{H}^+$ -specific *E. coli* subunit c has D61 at an equivalent position to *P. modestum* E65 and, by mutating residues around D61 to the corresponding ones from *P. modestum*, a  $\text{Li}^+$ -binding site is created (Zhang and Fillingame, 1995).

Subunit a is a very hydrophobic protein predicted to fold into five or six membrane-spanning  $\alpha$ -helices connected by short cytoplasmic and periplasmic loops (Yamada et al., 1996; Jäger et al., 1998; Long et al., 1998; Valiyaveetil and Fillingame, 1998). The only strictly conserved residue is R227 (*P. modestum* numbering), and no substitutions at this position permit ATP synthesis (Cain and Simoni, 1988; Lightowlers et al., 1987). According to the topology of subunit a, R227 is located near the cytoplasmic surface (Fig. 3A), where its electrostatic interaction with E65 of subunit c is likely. Subunit a contains almost no polar residues in the centre of the membrane, but some helices have a few polar residues in the flanking regions between the centre region and the two membrane surfaces. The helices may pack to allow for a water-filled channel in the centre that is open to the periplasm and closed on the cytoplasmic side. The areas with polar residues could contribute ion-binding sites to select for the specific permeation of the coupling  $\text{Na}^+$ ,  $\text{Li}^+$  or  $\text{H}^+$  across the channel. The accumulation of negatively charged amino acid residues in the loops is noteworthy (Fig. 3A,B). At the periplasmic side, these charges may contribute to separating the coupling cations from their anions to guide the former specifically into the mouth of the channel.

#### **$\text{Na}^+$ translocation through $F_0$ requires rotation of subunits c with respect to subunit a**

Experimental evidence for the specific recognition of the coupling  $\text{Na}^+$  by *P. modestum* subunit a has recently been obtained using a genetic approach. In the ATPase with the a subunit triple mutation (K220R, V264E, I278N),  $\text{Na}^+$  translocation was abolished, but  $\text{Li}^+$  or  $\text{H}^+$  translocation were retained (Kaim and Dimroth, 1998c). Using this mutant, insights of relevance for the ion translocation mechanism within the  $F_0$  motor were obtained. The starting point was the observation that ATP hydrolysis by the mutant enzyme was specifically inhibited by  $\text{Na}^+$ , in contrast to the wild-type ATPase which is activated by  $\text{Na}^+$ . Isotopic labelling experiments with  $^{22}\text{Na}^+$  have then shown that 1 mole of  $^{22}\text{Na}^+$  became occluded per mole of the mutant ATPase in a strictly ATP-dependent fashion (Kaim et al., 1998). The results are easily explained within the framework of the rotational mechanism and provide the first clear evidence for a rotation of the c subunit ring (rotor) with respect to subunit a (stator). First,  $^{22}\text{Na}^+$  binds readily from the aqueous environment to the c subunit binding sites; second, ATP hydrolysis promotes the rotation of the rotor with respect to the stator; this brings a rotor site occupied by  $^{22}\text{Na}^+$  into the interface with the stator channel. Since the channel is  $\text{Na}^+$ -impermeable (due to the mutation), the  $^{22}\text{Na}^+$  cannot dissociate from the rotor into the channel, and electrostatic constraints prevent the  $^{22}\text{Na}^+$ -occupied rotor site from rotating further out of the rotor–stator interface. Hence, ATP-driven rotation stops, and the rotor with one occluded  $^{22}\text{Na}^+$  at the interface to the stator channel is kept in an immobilised position. However, if a  $^{22}\text{Na}^+$ -bound rotor site approaches the wild-type channel, the  $^{22}\text{Na}^+$  dissociates

into the channel and passes through it to the periplasmic surface. This leads to a continued ATP-driven rotation coupled to  $\text{Na}^+$  accumulation on the periplasmic side of the membrane.

#### **The two operation modes of the $F_0$ motor**

We reasoned that, in the absence of an external energy source, the rotor should perform Brownian motion against the stator within a narrow angle. This idling motion of the motor is characterised by the exchange of internal unlabelled  $\text{Na}^+$  with external  $^{22}\text{Na}^+$  (Kaim and Dimroth, 1998b). Interestingly,  $\text{Na}^+_{\text{in}}/^{22}\text{Na}^+_{\text{out}}$  exchange was not significantly affected by modifying part of the rotor sites with DCCD. Therefore, an uninterrupted chain of rotor sites is not necessary to accommodate  $\text{Na}^+$  translocation by  $F_0$  across the membrane. Two different models for the  $F_0$  motor have been proposed, comprising either two or one stator half-channels. According to the two-channel model, an ion boards a rotor site through one stator channel and rides on it for almost a complete revolution until it is released through the second stator channel to the opposite side of the membrane (Junge et al., 1997). Clearly, the ion would never reach the second stator channel if the chain of rotor sites were interrupted by modification with DCCD. Hence, this model is not in accord with the evidence. In the alternative model with only one stator half-channel, the rotor site transfers the ion through this channel and releases it to the opposite side of the membrane after only minor rotation out of the interface with the stator (Dimroth et al., 1998). According to this proposal, the rotor sites outside the rotor–stator interface are in direct contact with the cytoplasm, whereas these sites are occluded in the alternative model.

The idling motor, characterised by  $^{22}\text{Na}^+_{\text{out}}/\text{Na}^+_{\text{in}}$  exchange, must switch into a torque-generating operation mode to perform work. This is accomplished by ATP-driven rotation of the  $\gamma$  subunit within the  $F_1$  module, which is linked to the rotation of the other rotor subunits and further to  $\text{Na}^+$  ( $\text{H}^+$ ) pumping across the membrane-bound  $F_0$  sector. If this rotation is induced in an ATP synthase with partially DCCD-modified rotor subunits,  $^{22}\text{Na}^+_{\text{out}}/\text{Na}^+_{\text{in}}$  exchange is abolished because ATP hydrolysis forces a DCCD-modified rotor subunit to strike against the stator and keeps it there in an immobilised position (Kaim and Dimroth, 1998b). In the reverse reaction, ATP synthesis requires rotary torque generated by the ‘downhill’ movement of the coupling ions across the  $F_0$  sector. Unexpectedly, this torque could not be generated with a  $\text{Na}^+$  concentration gradient ( $\Delta p\text{Na}$ ) alone. However, in the presence of a membrane potential ( $\Delta\psi$ ) with or without an additional  $\Delta p\text{Na}$ , the motor immediately switched from idling into the torque-generating mode, discontinuing  $^{22}\text{Na}^+_{\text{out}}/\text{Na}^+_{\text{in}}$  exchange (Kaim and Dimroth, 1998b).

This instructive result complements previous studies with the isolated  $F_0$  motor. This protein assembly catalysed  $^{22}\text{Na}^+_{\text{out}}/\text{Na}^+_{\text{in}}$  exchange but no unidirectional  $\text{Na}^+$  transport in the presence of large  $\Delta p\text{Na}$  values. For this transport mode, a membrane potential of at least  $-40\text{ mV}$  was essential, and at

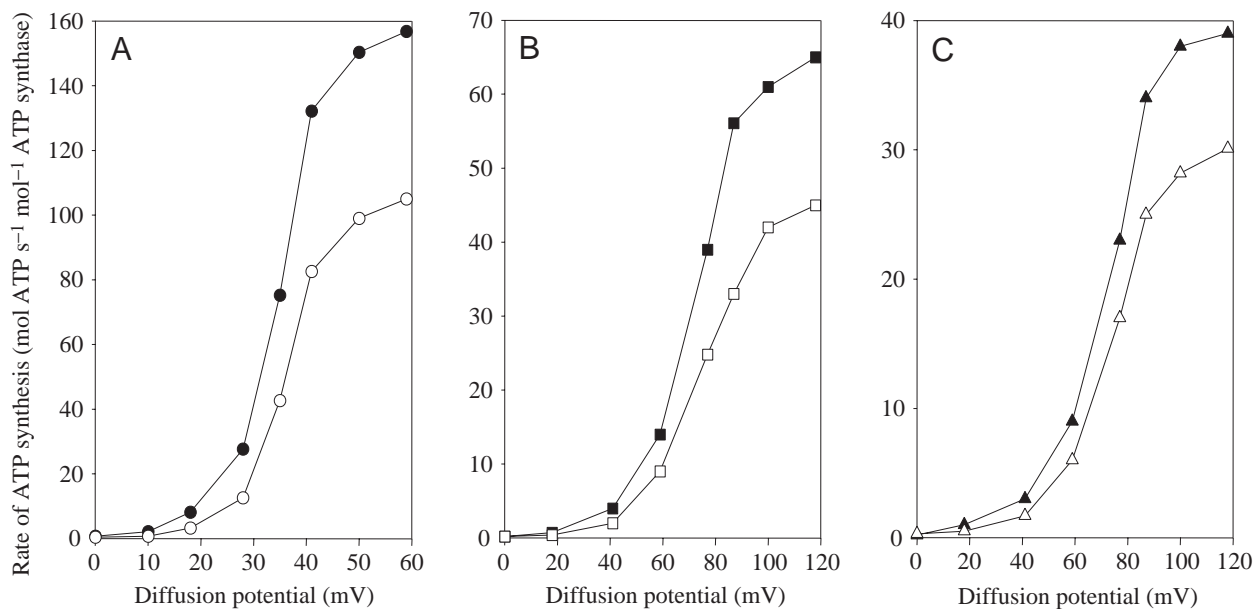


Fig. 4. Relative contribution of the electrical potential ( $\Delta\psi$ ) and the  $H^+$  or  $Na^+$  concentration gradient ( $\Delta pH$  and  $\Delta pNa$  respectively) to the rate of ATP formation by three different ATP synthases. (A) Reconstituted spinach chloroplast ATP synthase.  $K^+$ /valinomycin diffusion potentials were applied in the absence ( $\circ$ ) or presence ( $\bullet$ ) of  $\Delta pH=206$  mV. (B) Reconstituted *Escherichia coli* ATP synthase.  $K^+$ /valinomycin diffusion potentials were applied in the absence ( $\square$ ) or presence ( $\blacksquare$ ) of  $\Delta pH=206$  mV. (C) Reconstituted *Propionigenium modestum* ATP synthase.  $K^+$ /valinomycin diffusion potentials were applied in the absence ( $\triangle$ ) or presence ( $\blacktriangle$ ) of  $\Delta pNa^+=77$  mV (taken from Kaim and Dimroth, 1999).

higher potentials the velocity of  $Na^+$  transport was significantly increased (Kluge and Dimroth, 1992).

#### The obligatory role of the membrane potential for ATP synthesis

The obligatory role of the electrical potential ( $\Delta\psi$ ) for torque generation in the  $F_0$  motor of the ATP synthase strongly indicated that this force was also needed to produce ATP. This supposition has been verified using reconstituted ATP synthases from *P. modestum*, *E. coli* and spinach chloroplasts (Kaim and Dimroth, 1998a,b, 1999). In neither case was ATP synthesis observed if only an ion gradient ( $\Delta pNa^+$  or  $\Delta pH$ ) was applied (Fig. 4). The rate of ATP synthesis increased exponentially with increasing membrane potential, approaching saturation at  $\Delta\psi > 60$  mV for the chloroplast ATP synthase and at  $\Delta\psi > 120$  mV for the *P. modestum* and *E. coli* ATP synthases, respectively. The midpoint potential was approximately 30 mV for the ATP synthase from chloroplasts and approximately 70 mV for those from *P. modestum* and *E. coli*. Despite these differences, it is clear that the membrane potential is an indispensable driving force for all three ATP synthases. This is a surprising result, especially for the chloroplast enzyme, which has been reported to operate on  $\Delta pH$  alone (Jagendorf and Uribe, 1966). Furthermore, numerous studies seemed to indicate that  $\Delta pH$  and  $\Delta\psi$  provided not only thermodynamically but also kinetically equivalent driving forces for the synthesis of ATP (Junesch and Gräber, 1991; Turina et al., 1991). We noted in our recent studies, however, that the chemical concentration gradient ( $\Delta pH$  or  $\Delta pNa$ ) contributed to the rate of

ATP synthesis in all cases investigated, but far less than expected if  $\Delta\psi$  and  $\Delta pH$  ( $\Delta pNa$ ) were kinetically equivalent (Fig. 4) (Kaim and Dimroth, 1999).

These discrepancies could be traced back to the introduction of the 'succinate-bath method' for  $\Delta pH$  generation (Jagendorf and Uribe, 1966), which has been the method of choice ever since. First, chloroplasts were incubated with  $10 \text{ mmol l}^{-1}$  succinate, pH 4–5, to acidify the interior reservoir, and the  $\Delta pH$  was generated by subsequent 1:1 dilution into Tris buffer, pH 8.5. Unexpectedly, however, this method not only establishes the desired  $\Delta pH$  but also a  $\Delta\psi$  of appreciable size because of diffusion of the succinate monoanion (Kaim and Dimroth, 1998a, 1999). Immediately after the acid–base transition, the concentrations of the succinate monoanion in the acidic interior or the basic exterior are  $7.2 \text{ mmol l}^{-1}$  and  $0.006 \text{ mmol l}^{-1}$ , respectively. Diffusion of the charged succinate species across the membrane could therefore generate a Nernst potential of 180 mV. This is in reasonable agreement with the  $\Delta\psi$  of 140 mV determined experimentally (Kaim and Dimroth, 1999). The membrane permeability for the anionic succinate species probably increases significantly upon its folding into a ring in which the negative charge is delocalised to both carboxylic groups. Succinate, maleinate, malate or malonate, which can all adopt an intramolecular ring structure, develop a membrane potential in the 'acid-bath procedure', whereas fumarate with a *trans* double bond does not.

#### Model for torque generation in the $F_0$ motor

Fig. 5 shows a model of the  $F_0$  motor of *P. modestum* that

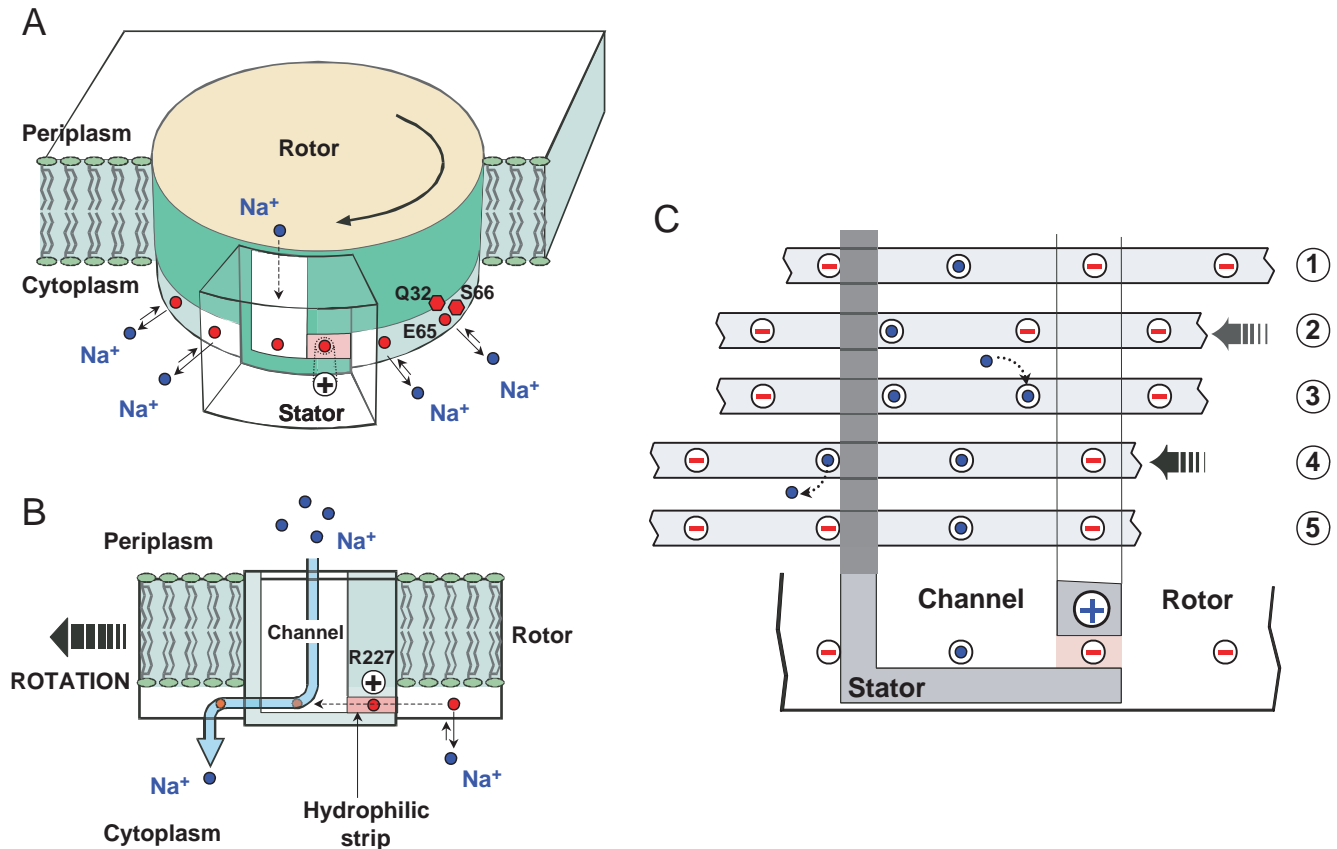


Fig. 5. (A) Diagrams of the rotor–stator assembly of the *Propionigenium modestum* ATP synthase. The rotor contains 9–12 Na<sup>+</sup>-binding sites near the cytoplasmic membrane surface. The stator contains an aqueous channel that conducts ions from the periplasmic reservoir to the level of the rotor sites. The channel is laterally connected with the cytoplasm by a hydrophilic strip. The positive stator charge (R227) prevents leakage of ions along this strip to the cytoplasm. (B) Face-on view of the rotor–stator assembly. Rotation during ATP synthesis is to the left. The stator channel admits Na<sup>+</sup> from the periplasm, but these ions can only exit to the cytoplasm by boarding a rotor site and passing through the dielectric barrier forming the left wall of the channel. (C) Typical sequence of events that advances the rotor by one step. In position 1, the third rotor site from the left has been captured by the stator charge. 1→2: the rotor site can escape from the potential well by thermal fluctuations, and the membrane potential biases its thermal escape to the left. However, it cannot pass the hydrophobic barrier that forms the left edge of the channel. 2→3: once the site has moved out of the potential well towards the channel, it picks up one Na<sup>+</sup>, which prevents its backwards attraction by the stator charge. 3→4: neutralised, the site no longer 'sees' the hydrophobic barrier and can diffuse to the left. Its motion is aided by the capture of the next rotor site by the stator charge, which pulls the rotor to the left. 4→5: emerging from the hydrophobic stator interface, the rotor site loses its ion to the cytoplasm. Now charged, it cannot diffuse backwards across the hydrophobic barrier, so the thermal motion to the left is ratcheted.

takes into account the experimental work mentioned in this article (Dimroth et al., 1999). The counter-rotating assemblies of the F<sub>o</sub> motor make up the rotor, consisting of a ring of 9–12 copies of subunits c, and the stator, comprising subunit a. The rotor contains the Na<sup>+</sup>-binding sites, consisting of the triad Q32, E65, S66 near the cytoplasmic surface of the membrane. To prevent ion leakage between the reservoirs, the entire rotor–stator interface is hydrophobic except for two regions: (i) an ion-selective blind channel within the stator that leads from the periplasm to the level of the rotor sites; and (ii) a hydrophobic strip that connects the channel laterally with the cytoplasmic reservoir. This permits charged (unoccupied) rotor sites to enter the rotor–stator interface from the right and to pass as far to the left as the edge of the stator channel. The universally conserved positive stator charge (R227) has been

placed close to this strip to prevent ions from leaking through this route to the cytoplasm. Having bound an ion from the channel, a rotor site can pass through the hydrophobic barrier and exit the stator, whereupon the site can discharge its ion to the cytoplasm. Hence, the flux of ions is from the periplasm through the stator channel onto an empty rotor site, and from there to the cytoplasm after the rotor has turned.

Now let us consider how this ion flux is coupled to the generation of rotary torque and what may be the fundamental role of the membrane potential in the torque-generating mechanism. Owing to random Brownian motion, the progression of the rotor is stochastic but, as a result of several electrostatic forces, its diffusion is biased to the left (Fig. 5). Let us start with a rotor site on the right edge of the stator interface. Occupation of this site is in dissociation equilibrium

with the cytoplasmic  $\text{Na}^+$  concentration. If the site is empty, it is electrostatically attracted with its negatively charged E65 by the positive stator charge R227. The captured site can escape by thermal fluctuations but, without the membrane potential, it is as likely to escape to the right as to the left. If the channel is aqueous, the bulk of the potential drop will be across the hydrophilic strip. This biases the thermal escape of the rotor site from its potential well to the left. Once in contact with the channel, the site will quickly pick up an ion, which reduces its electrostatic field to that of a dipole. This prevents it from being attracted backwards by the stator charge and enables it to pass easily through the hydrophobic barrier, when the next site diffuses into the stator and is captured by the stator charge. When the site emerges from the stator, it quickly loses its ion to the cytoplasm. With its negative charge, the site now encounters the dielectric barrier of the stator and cannot diffuse back to the right. Thus, the membrane potential plays the pivotal role in biased diffusion of the rotor to the left, which is essential for the generation of rotary torque. A low  $\text{Na}^+$  concentration on the cytoplasmic side accelerates rotation, because most rotor sites are empty and therefore attracted more frequently to the stator charge. A high  $\text{Na}^+$  concentration on the periplasmic side also accelerates rotation because an empty rotor site, having escaped from the stator charge to the channel, picks up a  $\text{Na}^+$  more quickly, and this favours its progression to the left. It is important to note that Oster and colleagues have made quantitative simulations of the motor's performance using the experimental data obtained from the *P. modestum* ATP synthase (Dimroth et al., 1999). These calculations show that the  $\text{Na}^+$   $F_0$  motor generates sufficient torque for ATP synthesis and that almost all the torque is due to the membrane potential.

### Future trends

Rapid progress has been made in the last few years in understanding the operating principles of the  $F_0$  motor of the ATP synthase. However, high-resolution structural information is lacking. The validity of our present working models needs to be checked with the structure to verify or falsify details of  $F_0$  function. A structure for  $F_0$  would undoubtedly also be extremely valuable in designing new experiments to answer specific questions about the motor's operation. For instance, it would be very rewarding to see the channel in the a subunit, the exact position of the stator charge R227, and the location of the rotor sites with respect to the membrane surface. Another unresolved problem is the connection of the c subunit ring to the other rotor subunits,  $\epsilon$  and  $\gamma$ . This will be important in understanding how rotational torque generated by the  $F_0$  motor is transmitted to the rotating parts within the  $F_1$  headpiece. Will the  $F_0$ -driven rotation of the  $\gamma$  subunit be continuous or will it proceed in three steps of  $120^\circ$  with an elastic spring in between? In what respects does the rotary  $F_0$  motor resemble the bacterial flagellar motor, and what are the differences?

The mechanochemistry and osmochemistry of the V-ATPases are further challenging problems for the future. The c subunit ring of this enzyme contains only half the number of binding

sites of the F-type ATPases. If F- and V-ATPases work on the same principle, twice as much ATP has to be consumed in the case of the V-ATPases to pump the same number of protons across the membrane; this obviously allows a steeper pH gradient to be generated. In the opposite direction, the  $V_0$  motor can use only every second rotor site for the torque-generating mechanism, so that, for ATP synthesis, the proton-motive force has to be substantially higher than for the F-ATPases. Many unresolved questions still have to be answered to understand in molecular detail how biological mechano-osmotic and mechanochemical energy-converting engines work.

### References

- Birkenhäger, R., Hoppert, M., Deckers-Hebestreit, G., Mayer, F. and Altendorf, K. (1995). The  $F_0$  complex of the *Escherichia coli* ATP synthase. Investigation by electron spectroscopic imaging and immunoelectron microscopy. *Eur. J. Biochem.* **230**, 58–67.
- Cain, B. D. and Simoni, R. D. (1988). Interaction between Glu-219 and His-245 within the a subunit of  $F_1F_0$ -ATPase in *Escherichia coli*. *J. Biol. Chem.* **263**, 6066–6612.
- Dimroth, P. (1997). Primary sodium ion translocating enzymes. *Biochim. Biophys. Acta* **1318**, 11–51.
- Dimroth, P., Kaim, G. and Matthey, U. (1998). The motor of the ATP synthase. *Biochim. Biophys. Acta* **1365**, 87–92.
- Dimroth, P., Wang, H., Grabe, M. and Oster, G. (1999). Energy transduction in the sodium F-ATPase of *Propionigenium modestum*. *Proc. Natl. Acad. Sci. USA* **96**, 4924–4929.
- Girvin, M. E. and Fillingame, R. H. (1994). Hairpin folding of subunit c of  $F_1F_0$  ATP synthase:  $^1\text{H}$  distance measurements to nitroxide-derivatized aspartyl-61. *Biochemistry* **33**, 665–674.
- Girvin, M. E., Rastogi, V. K., Abilgaard, F., Markley, J. L. and Fillingame, R. H. (1998). Solution structure of the transmembrane  $\text{H}^+$ -transporting subunit c of the  $F_1F_0$  ATP synthase. *Biochemistry* **37**, 8817–8824.
- Gräber, P. and Witt, H. T. (1976). Relations between the electric potential, pH gradient, proton flux and phosphorylation in the photosynthetic membrane. *Biochim. Biophys. Acta* **423**, 141–163.
- Hoffmann, A. and Dimroth, P. (1991). The electrochemical proton potential of *Bacillus alcalophilus*. *Eur. J. Biochem.* **201**, 467–473.
- Jagendorf, A. T. and Uribe, E. (1966). ATP formation caused by acid-base transition of spinach chloroplasts. *Proc. Natl. Acad. Sci. USA* **55**, 170–177.
- Jäger, H. F., Birkenhäger, R., Stalz, W.-D., Altendorf, K. and Deckers-Hebestreit, G. (1998). Topology of subunit a of the *Escherichia coli* ATP synthase. *Eur. J. Biochem.* **251**, 122–132.
- Junesch, U. and Gräber, P. (1991). The rate of ATP synthesis as a function of  $\Delta\psi$  catalyzed by the active, reduced  $\text{H}^+$ -ATPase from chloroplasts. *FEBS Lett.* **294**, 275–278.
- Junge, W., Lill, H. and Engelbrecht, S. (1997). ATP synthase: an electrochemical transducer with rotary mechanics. *Trends Biochem. Sci.* **22**, 420–423.
- Kaim, G. and Dimroth, P. (1993). Formation of a functionally active sodium-translocating  $F_1F_0$  ATPase in *Escherichia coli* by homologous recombination. *Eur. J. Biochem.* **218**, 937–944.
- Kaim, G. and Dimroth, P. (1998a). ATP synthesis by the  $F_1F_0$  ATP synthase of *Escherichia coli* is obligatorily dependent on the electric potential. *FEBS Lett.* **434**, 57–60.
- Kaim, G. and Dimroth, P. (1998b). Voltage-generated torque drives the motor of the ATP synthase. *EMBO J.* **17**, 5887–5895.



- Kaim, G. and Dimroth, P.** (1998c). A triple mutation in the a subunit of the *Escherichia coli/Propionigenium modestum* F<sub>1</sub>F<sub>o</sub> ATPase hybrid causes a switch from Na<sup>+</sup> stimulation to Na<sup>+</sup> inhibition. *Biochemistry* **37**, 4626–4634.
- Kaim, G. and Dimroth, P.** (1999). ATP synthesis by F-type ATP synthase is obligatorily dependent on the transmembrane voltage. *EMBO J.* **18**, 4118–4127.
- Kaim, G., Matthey, U. and Dimroth, P.** (1998). Mode of interaction of the single a subunit with the multimeric c subunits during the translocation of the coupling ions by F<sub>1</sub>F<sub>o</sub> ATPases. *EMBO J.* **17**, 688–695.
- Kaim, G., Wehrle, F., Gerike, U. and Dimroth, P.** (1997). Molecular basis for the coupling ion selectivity of F<sub>1</sub>F<sub>o</sub> ATP synthases: Probing the liganding groups for Na<sup>+</sup> and Li<sup>+</sup> in the c subunit of the ATP synthase from *Propionigenium modestum*. *Biochemistry* **36**, 9185–9194.
- Kluge, C. and Dimroth, P.** (1992). Studies on Na<sup>+</sup> and H<sup>+</sup> translocation through the F<sub>o</sub> part of the Na<sup>+</sup>-translocating F<sub>1</sub>F<sub>o</sub> ATPase from *Propionigenium modestum*: discovery of a membrane potential dependent step. *Biochemistry* **31**, 12665–12672.
- Kluge, C. and Dimroth, P.** (1993a). Kinetics of inactivation of the F<sub>1</sub>F<sub>o</sub> ATPase of *Propionigenium modestum* by dicyclohexylcarbodiimide in relationship to H<sup>+</sup> and Na<sup>+</sup> concentration: probing the binding site for the coupling ions. *Biochemistry* **32**, 10378–10386.
- Kluge, C. and Dimroth, P.** (1993b). Specific protection by Na<sup>+</sup> or Li<sup>+</sup> of the F<sub>1</sub>F<sub>o</sub> ATPase of *Propionigenium modestum* from the reaction with dicyclohexylcarbodiimide. *J. Biol. Chem.* **268**, 14557–14560.
- Krulwich, T. A.** (1995). Alkaliphiles: basic molecular problems of pH tolerance and bioenergetics. *Mol. Microbiol.* **15**, 403–410.
- Laubinger, W. and Dimroth, P.** (1988). Characterization of the ATP synthase of *Propionigenium modestum* as a primary sodium pump. *Biochemistry* **27**, 7531–7537.
- Lightowers, R. N., Howitt, S., Hatch, L., Gibson, F. and Cox, G. B.** (1987). The proton pore in the *Escherichia coli* F<sub>o</sub>F<sub>1</sub>-ATPase: a requirement for arginine at position 210 of the a subunit. *Biochim. Biophys. Acta* **894**, 399–406.
- Long, J. C., Wang, S. and Vik, S. B.** (1998). Membrane topology of subunit a of the F<sub>1</sub>F<sub>o</sub> ATP synthase as determined by labeling of unique cysteine residues. *J. Biol. Chem.* **273**, 16235–16240.
- Matthey, U., Kaim, G., Braun, D., Wüthrich, K. and Dimroth, P.** (1999). NMR studies of subunit c of the ATP synthase from *Propionigenium modestum* in dodecylsulfate micells. *Eur. J. Biochem.* **261**, 459–467.
- Matthey, U., Kaim, G. and Dimroth, P.** (1997). Subunit c from the sodium-ion-translocating F<sub>1</sub>F<sub>o</sub> ATPase of *Propionigenium modestum*. Production, purification and properties of the protein in dodecylsulfate solution. *Eur. J. Biochem.* **247**, 820–825.
- Neumann, S., Matthey, U., Kaim, G. and Dimroth, P.** (1998). Purification and properties of the F<sub>1</sub>F<sub>o</sub> ATPase of *Ilyobacter tartaricus*, a sodium ion pump. *J. Bacteriol.* **180**, 3312–3316.
- Singh, S., Turina, P., Bustamante, C. J., Keller, D. J. and Capaldi, R.** (1996). Topographical structure of membrane-bound *Escherichia coli* F<sub>1</sub>F<sub>o</sub> ATP synthase in aqueous buffer. *FEBS Lett.* **397**, 30–34.
- Takeyasu, K., Omote, H., Nettikadan, S., Tokumasu, F., Iwamoto-Kihara, A. and Futai, M.** (1996). Molecular imaging of *Escherichia coli* F<sub>1</sub>F<sub>o</sub>-ATPase in reconstituted membranes using atomic force microscopy. *FEBS Lett.* **392**, 110–113.
- Thayer, W. S. and Hinkle, P. C.** (1975). Synthesis of adenosine triphosphate by an artificially imposed electrochemical proton gradient in bovine heart submitochondrial particles. *J. Biol. Chem.* **250**, 5330–5335.
- Turina, P., Melandri, B. A. and Gräber, P.** (1991). ATP synthesis in chromatophores driven by artificially induced ion gradients. *Eur. J. Biochem.* **196**, 225–229.
- Uribe, E.** (1973). ATP synthesis by a K<sup>+</sup>-valinomycin-induced charge imbalance across chloroplast grana membranes. *FEBS Lett.* **36**, 143–147.
- Valiyaveetil, F. I. and Fillingame, R. H.** (1998). Transmembrane topology of subunit a in the *Escherichia coli* F<sub>1</sub>F<sub>o</sub> ATP synthase. *J. Biol. Chem.* **273**, 16241–16247.
- Yamada, H., Moriyama, Y., Maeda, M. and Futai, M.** (1996). Transmembrane topology of *Escherichia coli* H<sup>+</sup>-ATPase subunit a. *FEBS Lett.* **390**, 34–38.
- Zhang, Y. and Fillingame, R. H.** (1995). Changing the ion binding specificity of the *Escherichia coli* H<sup>+</sup>-transporting ATP synthase by directed mutagenesis of subunit c. *J. Biol. Chem.* **270**, 87–93.